Environment and Natural Resources Journal

Volume 24
Issue 2
2026

Circular Economy Pathway: Valorization of Cotton Stalk into Biochar for Textile Wastewater Treatment

Vishwa Vraj Shah[1] and N. M. Patel[2*]

[1]*Research Scholar, Environmental Engineering, Gujarat Technological University, Ahmedabad, India*
[2]*Chemical Engineering Department, Government Engineering College Valsad-3960001, Gujarat, India*

ARTICLE INFO

Received: 14 Oct 2025
Received in revised: 10 Dec 2025
Accepted: 19 Dec 2025
Published online: 28 Jan 2026
DOI: 10.32526/ennrj/24/20250255

Keywords:
Circular economy/ Phosphate modified cotton stalk biochar/ Multicomponent synthetic textile wastewater/ COD removal/ Adsorption kinetics/ Langmuir isotherm

*** Corresponding author:**
E-mail: prof.nmpatel@gmail.com

ABSTRACT

Agricultural residues, often burned openly pose environmental challenges but offers opportunities for valorization into functional materials. Converting such residues into biochar supports circular economy principles. Here, cotton stalk (CS) was converted into phosphate-modified biochar (PMCS) via pyrolysis at 350, 550, and 800°C. Response Surface Methodology (RSM) was applied to the adsorption process, treating pyrolysis temperature as a categorical factor in a rotatable CCD. PMCS was characterized by Brunauer-Emmett-Teller (BET), Scanning Electron Microscopy (SEM), and Fourier Transform Infrared Spectroscopy (FTIR), Point of Zero Charge while adsorption was evaluated through isotherm and kinetic modeling for synthetic textile wastewater containing Eriochrome Black T (EBT), starch, and salts. PCS800 exhibited a BET analysis of 750 m² per gram of biochar and achieved nearly 77% COD reduction at 33 min and 6.43 g/L for synthetic wastewater, while 60% with complete decolorization for real effluent. The optimum removal followed Langmuir behaviour (q_{max}=90.2 mg/g, K_L= 0.049 L/mg) with pseudo-second-order kinetics, reflecting micropore filling by starch. Overall, this study establishes a circular economy pathway by valorizing CS into an efficient adsorbent, mitigating residue burning while offering scalable potential for textile wastewater treatment.

HIGHLIGHTS

- Cotton stalk was valorized into phosphate-modified biochar via pyrolysis.
- Adsorption shifted from Freundlich multilayer to Langmuir monolayer at 800°C.
- PCS800 achieved 77% COD reduction for multicomponent synthetic water and 60% removal for real textile effluent.
- PCS550 provided balanced adsorption of both small and large organic molecules.
- Study supports circular economy by converting residues into functional adsorbents.

1. INTRODUCTION

Water is increasingly recognized not only as a vital resource but also as a reservoir of recoverable materials, a perspective central to the circular economy in wastewater management. Wastewater is no longer viewed solely as waste but as a source of nutrients, energy, and reusable materials (Tzanakakis et al., 2023; Agyemang et al., 2024). Within this framework, valorizing agricultural residues into functional materials offers a sustainable pathway for resource recovery. Biochar, produced through thermal conversion of biomass, exemplifies this approach: its porous structure and reactive surface chemistry enable efficient adsorption of dyes, heavy metals, and organics (He et al., 2022), while simultaneously recycling biomass that would otherwise drive environmental degradation (Xiang et al., 2022). Thus, biochar use in wastewater treatment unites pollution control with resource recovery, advancing circular economy principles (Colmenares et al., 2016).

Each year, India generates nearly 87.0 million tonnes of agro residues and their open field burning remaining the dominant disposal method that contributed to air pollution surpassing levels reported in other Asian countries. Where, India is also the second-largest contributor to carbon aerosol emissions, releasing approximately 84 teragram per year (Bhuvaneshwari et al., 2019; Grover and

Citation: Shah VV, Patel NM. Circular economy pathway: Valorization of cotton stalk into biochar for textile wastewater treatment. Environ. Nat. Resour. J. 2026;24(2):250-267. (https://doi.org/10.32526/ennrj/24/20250255)

Chaudhry, 2019; Dhanya, 2022). Among these, cotton stalk (CS) is a major agro-residue (Deshpande et al., 2023). This study establishes a closed-loop framework where CS residues from the textile sector are valorized into phosphate-modified biochar to mitigate the very pollution burden generated by that sector Figure 1.

The textile sector that is considered as a key pillar of the Indian economy, generate approximately 140-200 L of wastewater per kilogram of fabric with high organic load (Arous et al., 2024). The World Bank identifies it as a major environmental challenge, with dyeing and finishing alone contributing 17%-20% of industrial effluents (Okafor et al., 2021). These effluents contain dyes, chromium, alkalis, and acids (Sathya et al., 2022), among which persistent azo dyes e.g., benzene diazonium chloride derivatives, Naphthoic acid derivatives, Reactive Green 19, Eriochrome Black T are particularly concerning due to their transformation into mutagenic and carcinogenic aromatic amines (Sadeghi et al., 2021; Ali et al., 2022). Beyond dyes, textile wastewater also carries additives such as starch and salts, which significantly contribute to the Chemical Oxygen Demand (COD), a critical parameter in environmental management.

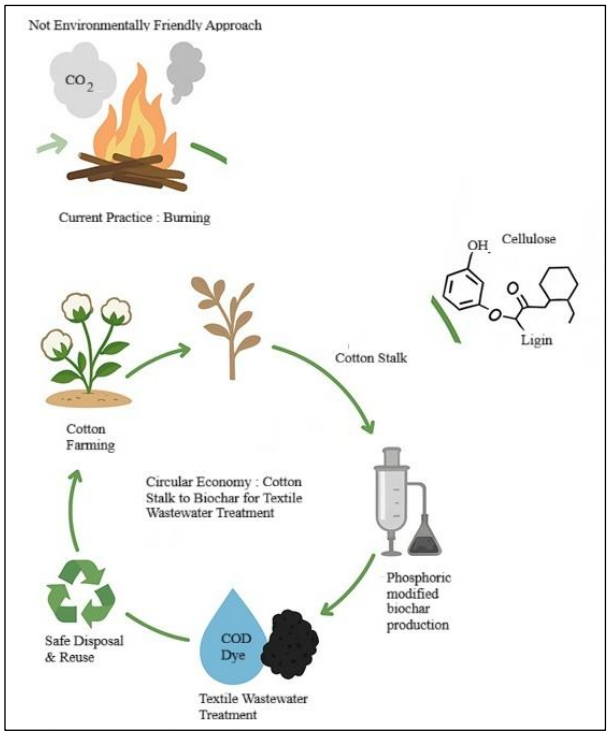

Figure 1. Circular economy approach for cotton stalk biochar

Conventional treatment technologies often prove inadequate for such complex pollution. Biochar offers a circular economy based solution, enabling effective contaminant removal and resource recovery while addressing biomass waste challenges (Wu and Wu, 2019; Kwarciak-Kozłowska and Fijałkowski, 2021). CS is a rich in cellulose, hemicellulose, and lignin, decomposes thermally into a stable aromatic matrix with micropores suitable for adsorption (Zhao et al., 2022; Zhu et al., 2022; Cui et al., 2024). Till date thermally prepared CS biochar preliminary utilized for heavy metal removal form water, achieving removal efficiencies of >80% (Cr^{+6}), 80.90 µg/g (As) and 146.78 mg/g for Pb^{+2} for pyrolysis temperature between 400-550°C (Hussain et al., 2020; Gao et al., 2021; Ahmad et al., 2022; Khalid and Inam, 2024). In contrast, Shah et al. (2022) reported a relatively lower adsorption capacity of 30-40 mg/g for Malachite green dye at 100 mg/L by unmodified CS. However, modified CS with H_3PO_4 acid enhanced dye removal capacity of 144.36 mg/g for RhB dye with >99.5% removal (Venkatesan et al., 2025). Similar improvements have been observed for agro waste derived biochar treated with H_3PO_4 such as coconut shell [95.4% MB removal, (Xu et al., 2023)], sugarcane bagasse [357.14 mg/g, (Zhou et al., 2022)], and corn straw [251.08 mg/g, (Liu et al., 2024)]. Recent advances therefore emphasize heteroatom modification particularly with phosphorus incorporation which substantially alters physicochemical properties, introducing unique surface functionalities (Tan et al., 2022; Xu et al., 2024; Zafar et al., 2024). Phosphorus modification restructures functional groups, increases graphite defect density, and enhances adsorption of diverse pollutants (Ou et al., 2023; Li et al., 2024b; Li et al., 2024a; Zeng et al., 2024). It also introduces acidic sites, improves stability, and markedly increases affinity for metal ions and alkaline organics (Arampatzidou et al., 2017; Liu et al., 2021; Shao et al., 2024; Du et al., 2025).

This study addresses a key research gap in textile wastewater treatment by developing a circular economy pathway for valorizing cotton stalk into phosphate-modified biochar (PMCS) under multi-component wastewater conditions. PMCS produced at 350, 550, and 800°C was characterized by Brunauer-Emmett-Teller (BET), Scanning Electron Microscopy (SEM), and Fourier Transform Infrared Spectroscopy (FTIR), Point of Zero Charge and evaluated for COD removal using a novel Response surface Methodology (RSM) framework that treats pyrolysis temperature as a categorical factor in a rotatable central composite design (CCD). Inclusion of RSM in adsorption process enables the development of statistically reliable

quadratic models while capturing curvature and interaction effects in the response surface. RSM provides a resource efficient alternative to traditional experimental approaches because it identifies optimal operating conditions using fewer experimental runs and simultaneously evaluates both main and interaction effects (Susaimanickam et al., 2023).

The adsorption efficiency is influenced by several interacting parameters, including pH, adsorbent dose, mixing time, temperature, and initial contaminant concentration (Yaseen and Scholz, 2019). Conventional one-variable-at-a-time (OVAT) methods fail to capture such interactions, are labour intensive, and provide limited insight into overall process behaviour in traditional RSM frame work (Dowlatshah et al., 2025). Hence, use of RSM in present study offers advantage to maximize the pollutant reduction by optimizing the operating parameters. Till date, limited studies have successfully employed RSM (CCD/BBD) to optimize adsorption parameters for COD and BOD removal processes using biosorbents and activated materials (Oyekanmi et al., 2019; Manzar et al., 2021; Roy et al., 2022).

By contrast, the RSM-CCD approach extends the conventional RSM framework by combining continuous and categorical inputs, enabling detailed assessment of how structural and functional biochar properties interact with process parameters. Furthermore, kinetic and isotherm modeling were employed to elucidate the governing adsorption mechanisms As highlighted by (Srivastav et al., 2024) such multi-pollutant evaluation is critical for scale-up. Hence, the study shows that phosphorus modification and pyrolysis markedly enhance adsorption efficiency and explain the mechanisms involved in multicomponent system. Moreover, this work provides a viable pathway for converting biomass into effective materials for feasible wastewater treatment in real world. Therefore, this approach offers a practical and cost-effective means for biomass utilization and cleaner wastewater management leads to circular economy concept in textile sector.

2. METHODOLOGY

2.1 Multi component synthetic textile wastewater

A synthetic wastewater representative of textile effluent was prepared to simulate partially treated effluent. Eriochrome Black-T (EBT, 30 mg/L) was obtained from a textile unit in Ahmedabad, while starch (250 mg/L), Na_2CO_3 (100 mg/L), $NaHCO_3$ (100 mg/L), NaCl (150 mg/L), NaOH (50 mg/L), and H_2SO_4 (30 mg/L) were laboratory grade reagents (Merck, India; >90% purity). Constituents were sequentially dissolved in distilled water under stirring (200 rpm, 30 min) to obtain a homogeneous dark-blue solution of neutral pH, consistent with actual effluent. The COD was 220±10 mg/L and BOD of 50±5 mg/L, having BOD:COD ratio of 0.23 which is <0.3 considered as non-biodegradable in nature (Muhammad et al., 2008). Fresh synthetic wastewater was prepared for each experiment to maintain reproducibility.

2.2 Synthesis of phosphate modified cotton stalk biochar (PMCS)

About 100 kg of cotton stalk (CS) was collected from farms near Himmantnagar, Gujarat, cut into 2-3 cm pieces, rinsed thoroughly with distilled water (DW) and subsequently dried for 4 h under sunlight. A 100 g batch was chemically activated by adding in 85% Phosphoric acid solution at a 0.5:1 ratio (CS:acid, w/w) under stirring for 1 h, then oven-dried at 110°C for 48 h. The precursor was subjected to thermal treatment in a muffle furnace at 350, 550, and 800°C for 2 h (heating rate 10°C/min, limited oxygen). Once cooled the biochar rinsed repeatedly with hot DW and neutralized with NaOH till pH of the rinse water pH reached 7, followed by drying in an oven at 105°C for 12 h. The dried product less than 0.5 mm kept in seal container. The synthesized samples were denoted PCS350, PCS550, and PCS800. A synthesis pathway is shown in schematic form in Figure 2.

2.3 Characterization of Phosphate Modified Cotton Stalk Biochar (PMCS)

Biochar PCS350, PCS550, and PCS800 were characterized to assess changes in surface morphology, functional groups, and pore structure across pyrolysis temperatures. The BET analysis, point of zero charge, SEM, and FTIR analyses were performed to evaluate surface area, charge, morphology, and functionalities, respectively. BET was measured using a Surface Area Analyzer (Test method: IKC/ACC/INS09/BET) at the Advanced Characterization Centre, Ashapura Mine Chem, Gujarat. Point of zero charge was determined by the pH drift method. SEM was conducted at the Central Instrumentation Facility, Central University of Gujarat (Model: EVO 18, Carl Zeiss), and FTIR spectra (400-4,000 cm^{-1}) recorded with a Perkin Elmer SP-65 using KBr pellets. Optimized biochar showing maximum

COD removal was further analyze with advanced SEM and FTIR for validation.

2.4 Optimization study for COD reduction using RSM.

RSM was adopted to enhance COD removal efficiency by analyzing the effects of adsorbent dose and mixing time, while treating pyrolysis temperature (350, 550, 800°C) as a categorical factor. This approach extends the conventional RSM framework by combining continuous and categorical inputs, enabling detailed assessment of how structural and functional biochar properties interact with process parameters. Experiments were conducted at pH 7 and 400 rpm under ambient conditions. A Face-Cantered Central Composite Design (CCD) was adopted with two continuous factors (dose, time) and one categorical factor (temperature). The factor ranges are summarized in Table 1.

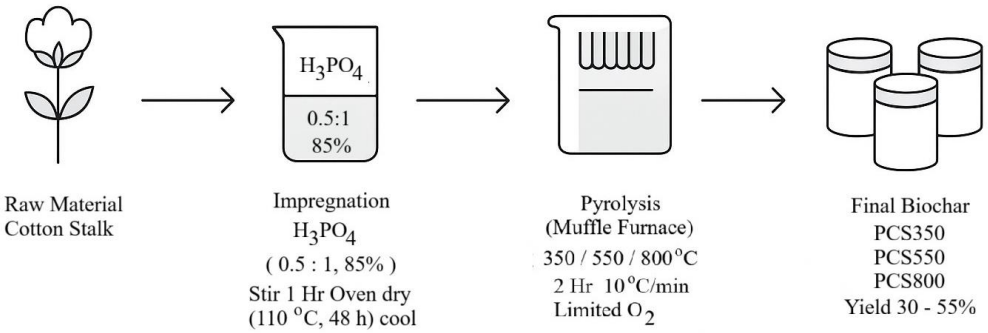

Figure 2. Phosphate modified CS biochar synthesis process

Table 1. RSM-CCD framework for optimization

Independent variables	Factor	Unit	Low	Centre	High
Adsorbent dose (PCS350, PCS550, and PCS800)	A	g/L	0.1	5.25	10
Mixing time	B	min	5	27.5	50
Pyrolysis temperature	L1, L2, L3	°C	350	550	800

The general formula for CCD is as (Equation 1). Where, k=number of continuous variables (here k=2), 2^k=no. of factorial points, 2k=star points, n_c=number of centre points (with replicates) and L=number of categoric levels.

$$N = (2^k + 2k + n_c) \times L \quad (1)$$

Hence, The CCD has developed 33 runs in Design of Experiment (DoE) covering factorial points, axial points, and replicated centre points, distributed across the three pyrolysis temperatures (350, 550, and 800°C) as categoric level. The datasets were analyzed and expressed through a second-order polynomial Equation 2):

$$Y = \beta_0 + \beta_1X_1 + \beta_2X_2 + \beta_3D_1 + \beta_4D_2 + \beta_{11}X_{12} + \beta_{22}X_{22} + \beta_{12}X_1X_2 + \beta_{13}X_1D_1 + \beta_{14}X_1D_2 + \beta_{23}X_2D_1 + \beta_{24}X_2D_2 \quad (2)$$

Where; Y is % COD reduction, X1 and X2 are dose and time, and D1, D2 are dummy variables for temperature. Model adequacy was assessed by ANOVA, and regression effects were visualized through 3D response surfaces. Design-Expert® software (v23.1.6, Stat-Ease Inc., USA) was implemented for optimization.

2.5 Isotherm study

Equilibrium adsorption of COD by phosphate-modified cotton stalk (PMCS) biochar was evaluated at the optimized mixing time and initial COD from the RSM study. Different adsorbent doses were tested, once equilibrium was attained COD_f was analyze to determine the uptake capacity q_e (in mg/g) using (Equation 3);

$$q_e = \frac{(Ci - Ce) * V}{W} \quad (3)$$

Where; C_i (initial) and C_e (equilibrium) concentration of COD (in mg/L), V is volume (in L), and W (adsorbent mass, in g).

To interpret the adsorption process, the data were modelled with Langmuir and Freundlich adsorption isotherm equations. According to the Langmuir model, adsorption is restricted to single monolayer, which is represented as (Equation 4) and Freundlich Model describe heterogenous adsorption and is represented as (Equation 5).

Langmuir Model:

$$\frac{1}{qe} = \frac{1}{qm} + \frac{1}{qmb} \times \frac{1}{Ce} \quad (4)$$

Freundlich Model:

$$\ln (qe) = \ln (k_f) + \frac{1}{n} \ln (Ce) \quad (5)$$

The adsorption constants (a, b, K_f, n) were determined from the respective linear plots, the degree of fit for each model was evaluated with R^2.

2.6 Kinetic study

Adsorption kinetics of COD on PMCS biochar (PCS350, PCS550, PCS800) were studied at optimized dose and initial COD. Batch tests were run at 400 rpm with contact times of 5-180 min. COD was measured at each interval, and the adsorption capacity at given time q_t (mg/g) was determined as per (Equation 6).

$$q_t = \frac{(Ci - Ct) \times V}{W} \quad (6)$$

Where; C_i (initial) and C_t (t, time) COD concentration where, V (in L) is the solution volume, and W (in g) is the mass of biochar. The kinetic data were modelled using pseudo first order (Equation 7) and pseudo-second-order (Equation 8) equations;

Pseudo-1st-Order (PFO) Model:

$$\ln (qe - qt) = \ln qe - k_1 \times (t) \quad (7)$$

Here, q_e (in mg/g) corresponds to adsorption capacity at equilibrium, q_t (in mg/g) indicates adsorption time (t), while k_1 (min^{-1}) is defined well by the pseudo-first-order rate constant.

Pseudo-2nd-Order Model:

$$\frac{t}{qt} = \frac{1}{k2 \times qe^2} + \frac{t}{qe} \quad (8)$$

Where; k_2 (g/mg·min) is the pseudo-second-order rate constant.

3. RESULTS AND DISCUSSION

3.1 BET and SEM analysis results at varied temperature

The available surface per unit mass and morphology of PMCS biochar were greatly influenced by pyrolysis temperature because of structural transition. Values increased from 180 (m^2/g, PCS350) to 450 (m^2/g, PCS550) and 750 (m^2/g, PCS800) due to increase in pore size and volume (Table 2). This enhancement results from devolatilization, where volatile loss leaves a porous carbon skeleton (Díaz et al., 2024). Similar correlations between temperature and pore development have been reported for cotton stalk (300-700°C) and wheat straw (700°C, 400 m^2/g, pore size 2.34 nm) (Muzyka et al., 2023). The highly porous PCS800 facilitates diffusion of dyes and macromolecules such as starch during adsorption.

Table 2. Results of surface area (BET) analysis

Biochar	SBET (m^2/g)	Pore size (Å)	Pore size (in nm)	Pore volume (cm^3/g)
PCS 350	180	14.7985	1.4	0.0193
PCS 550	450	18.5654	1.8	0.0564
PCS 800	750	22.4588	2.2	0.0835

Phosphoric acid activation further promotes pore formation through structural swelling and amplification, explaining the higher porosity in PMCS compared to unmodified biochar (Zhao et al., 2017). Networks were observed in KOH-activated cotton stalk at 900°C.

SEM images of PCS800 at low (5.0 KX) and high (10.0 KX) magnification (Figure 3) reveal hollow, elongated pores that facilitate transport of COD contributing solutes. Similar mesoporous For H_3PO_4 treated biochar, micro/mesopores and fractured sheet-like surfaces have also been reported (Cui et al., 2024) supporting enhanced adsorption performance (Du et al., 2025).

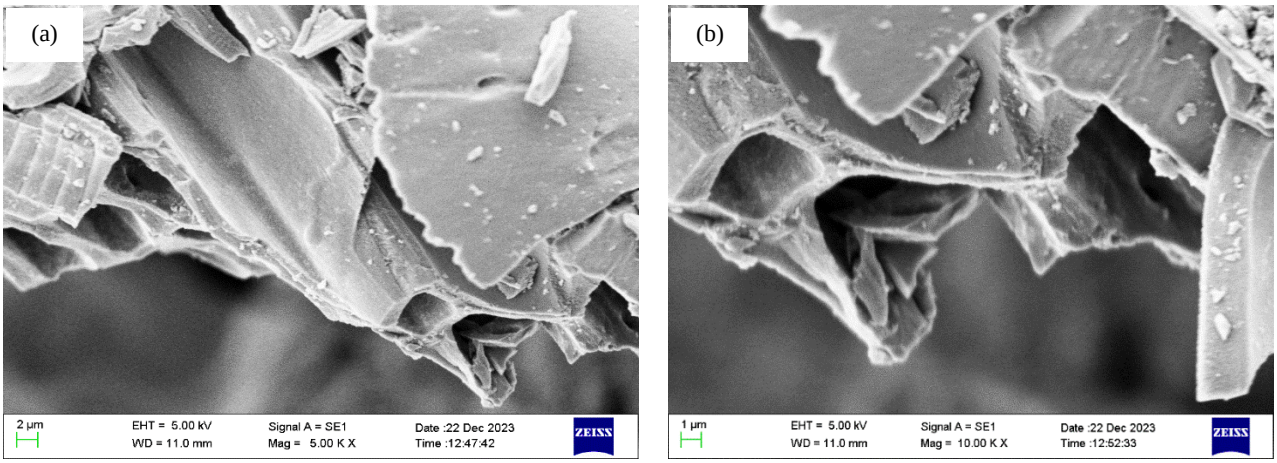

Figure 3. SEM images of PCS800 at (a) low (5.0 KX) and (b) High (10.0 KX) magnification

3.2 Results of change in surface functionality at varied temperature by FTIR

The spectra of PMCS biochar prepared at 350, 550, and 800°C (Figure 4(a-c)) showed a systematic development of surface functionalities with temperature. All the biochar showed deoxygenation and aromatization with redistribution of phosphate functionalities explain the transition from hydrogen bond dominated interactions to π-π interactions on more graphitized domains and phosphate modified biochar as mentioned in Table 3.

Here, FTIR graphs showed of carbonyl groups, weakening of aliphatic C-H, and stabilization of phosphate functionalities with increasing pyrolysis temperature. Phosphoric acid treated rice husk has also been documented the same results for weakening of C-H bands at higher pyrolysis temperature (Zeng et al., 2022). Whereas walnut shell (Heidarinejad et al., 2020), and sugarcane bagasse derived biochar (Kamran et al., 2022) has resulted that confirming that phosphate activation governs both surface chemistry and thermal stability across diverse biomass precursors.

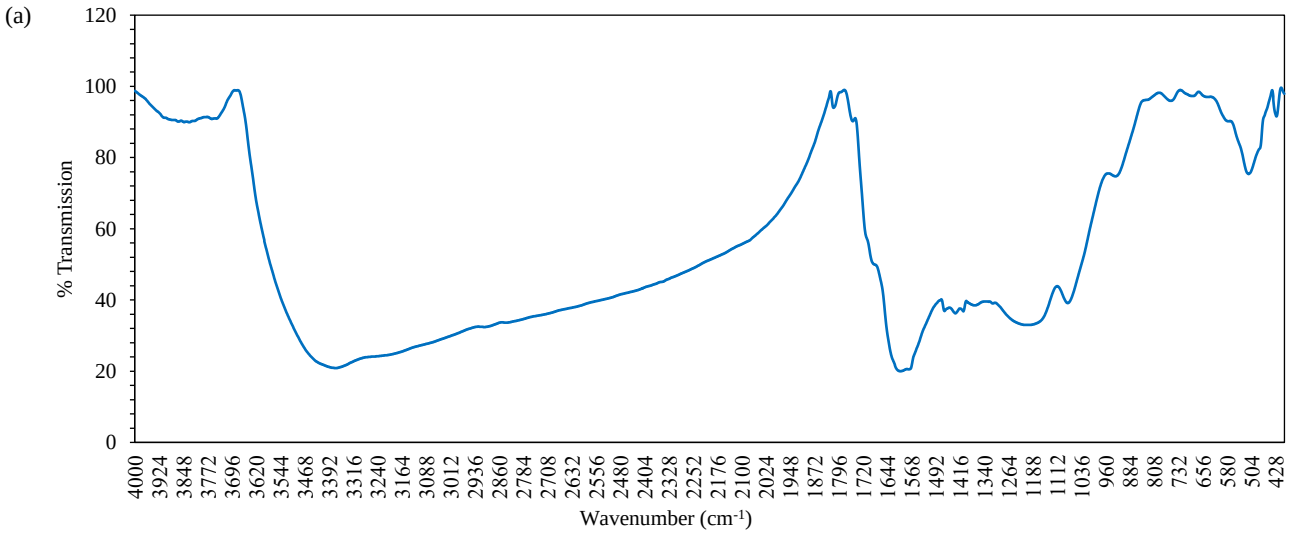

Figure 4. FTIR graph of phosphate modified cotton stalk biochar (a) PCS350, (b) PCS550, (c) PCS800

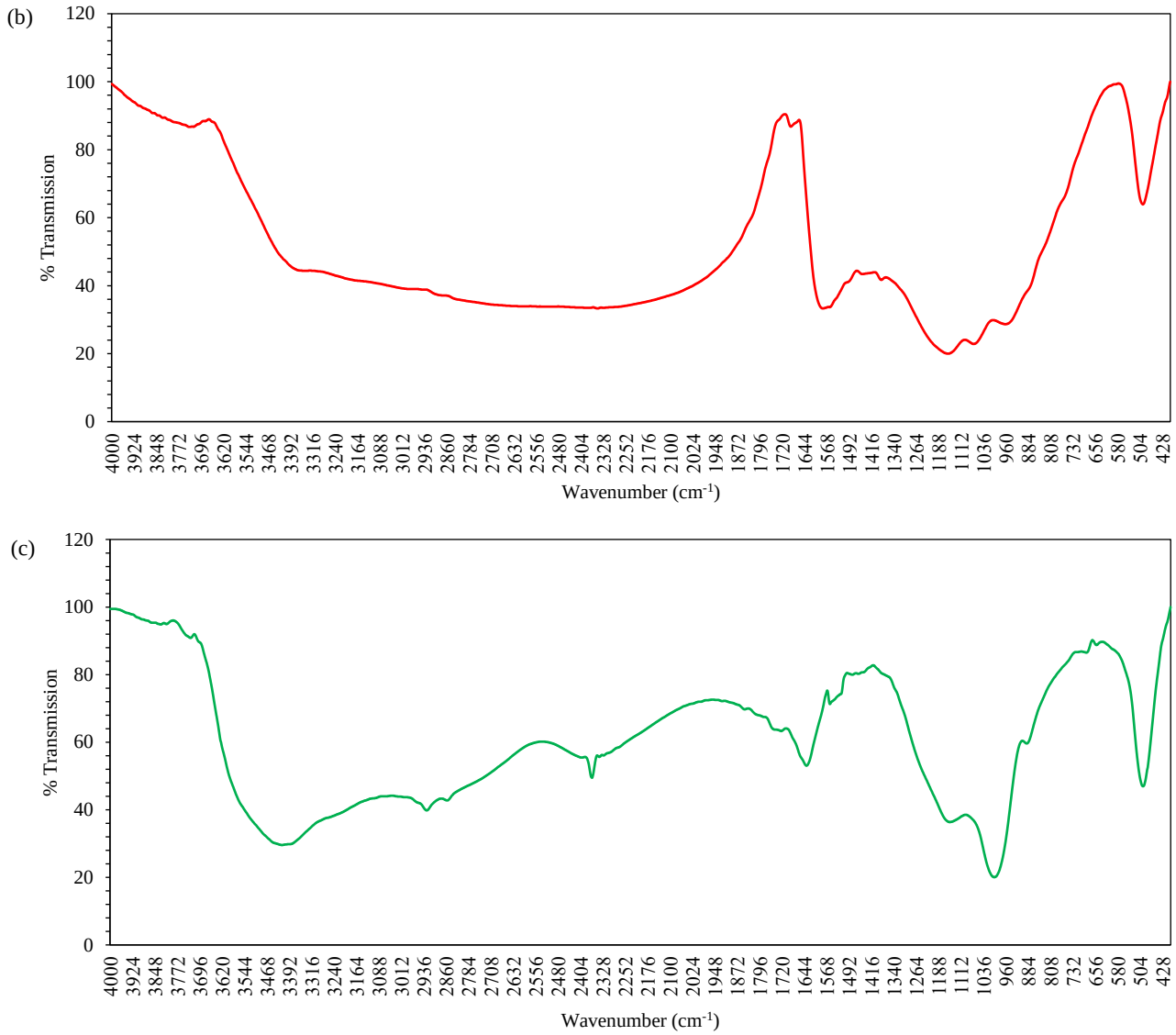

Figure 4. FTIR graph of phosphate modified cotton stalk biochar (a) PCS350, (b) PCS550, (c) PCS800

Table 3. Change in the functional groups in phosphate modified cotton stalk derived biochar

Wavenumber (cm^{-1})	Functional group	PCS350	PCS550	PCS800	Key process
3,300-3,500	O-H / N–H stretching	Strong (3370)	Narrow, shifted (3758)	Weak (3416)	De-hydroxylation, loss of H-bonding
2,925-2,850	Aliphatic C-H	Present	Reduced	Absent	Chain cracking, aromatization
1,700-1,800	C=O stretching	Present (1690)	Weakened (1636)	Absent	Decarboxylation, conjugation
1,580-1,620	Aromatic C=C	Weak	Stronger (1590)	Strong (1556)	Aromatization, ring condensation
1,400-1,450	C-H / phenolic O-H	Present (1445)	Reduced	Absent	Phenolic loss, condensation
1,150-1,200	P=O stretching	Present (1155)	Strong (1156)	Shifted (1148)	Phosphorylation, esterification
1,000-1,070	P-O-C stretching	1037	1068	998	Phosphate-C bonding, stabilization
~915	P-O-P (pyrophosphate)	Absent	Weak	Strong	Polycondensation, pyrophosphate
750-760	Aromatic C-H bending	Present	Present	Retained	Aromaticity, graphitization

3.3 Model performance and factor effects

The results of the total 33 results of experiments designed as per (Equation 2) are provided as supplementary material (Table S1) with this manuscript. Among various tested models, the quadratic model suggested by Design-Expert 23.1.6.0 was selected based on its superior statistical fit. The regression analysis yielded high coefficients of determination (R^2=0.9897, adjusted R^2=0.9897, and predicted R^2=0.9828), with less than 2% difference between adjusted and predicted R^2, confirming the adequacy of the model (Khan et al., 2021; Yusuff et al., 2023). The strong correlation between experimental and predicted COD reduction is mentioned in scattered plot Predicted vs actual for % COD reduction Figure 5, supporting the robustness of the quadratic equation (Equation 9) for process predictions.

$$\% \text{ COD Reduction} = 55.65 + 5.97\,A + 8.28\,B - 14.84\,C[1] - 2.90\,C[2] - 0.0417\,AB + 1.86\,AC[1] - 1.89\,AC[2] + 2.31\,BC[1] - 2.19\,BC[2] - 2.09\,A^2 + 1.33\,B^2 \quad (9)$$

The regression coefficients revealed that adsorbent dose (A) and mixing time (B) had significant positive effects on COD reduction, while the quadratic term of adsorbent dose was negative, indicating diminishing efficiency at higher levels. This trend is consistent with earlier adsorption studies reporting overdosing effects due to aggregation and active site masking (Beyan et al., 2021; Vakili et al., 2023). Interaction terms indicated that the adsorbent dose and mixing time (AB) interaction was antagonistic, while mixing time and temperature (BC) showed a synergistic effect. Here mixing time is the most crucial parameter, which aligns with previous reports highlighting the importance of contact time for molecular transport in adsorption studies. (Soleimani et al., 2023).

3.4 ANOVA results and model adequacy

The quadratic model was assessed through ANOVA (Table 4), and the results demonstrated the strong statistically significance ($p<0.0001$), that showed the selected factors adequately explained the observed variability in COD reduction. The adsorbent dose (A) and mixing time (B) alone and their quadratic terms were highly significant, while interaction effects AB have $p>0.05$ that is non-significant and negligible effect on COD removal. Since the lack of fit test returned $p>0.05$, the residual error was considered random supporting the adequacy of model in representing the observed data.

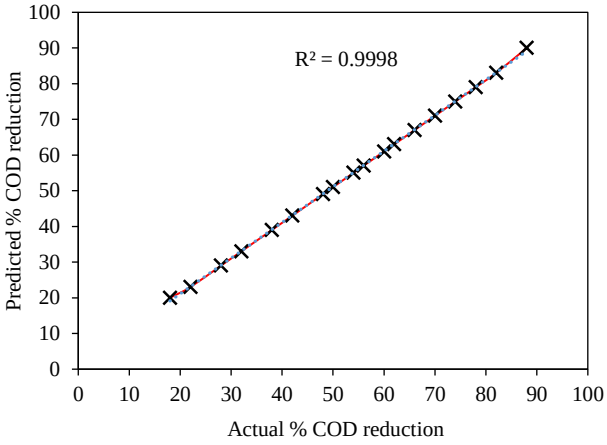

Figure 5. Scattered plot predicted vs actual for % COD reduction

3.5 Response surface evaluation by 3D plot

The three-dimensional response surface plots illustrated in Figure 6(a-c) the collective effects of adsorbent dose and mixing time on variation in COD reduction at different pyrolysis levels. COD removal increased with adsorbent dose but plateaued at higher values, indicating site saturation. Mixing time also enhanced removal, particularly at intermediate doses, highlighting its role in mass transfer. For PCS350 as per Figure 6(a), maximum COD removal reached between 55-60%, with a relatively flat surface suggesting a near-linear relationship between dose and time. PCS550 as showed in Figure 6(b) a flatter surface, indicating equilibrium conditions with limited improvement beyond approx. 62%. In contrast, PCS800 as per Figure 6(c) displayed strong positive interactions of dose and mixing time, achieving >80% COD removal at 10 g/L and 50 min.

These plots confirm the influence of pyrolysis temperature on adsorbent properties governing multicomponent adsorption. PCS800 achieved the highest efficiency (76.7% COD removal at 6.43 g/L, 33 min), while PCS550 offered balanced performance. Comparable studies, such as sugarcane bagasse activated carbon (96% COD removal at optimized conditions), also emphasize pH as a key factor (Beyan et al., 2021).

Table 4. ANOVA output of model

Factor	Sum of squares (SS)	Degree of freedom (df)	Mean square (MS)	F-ratio	Probability (P)
Model	7,995.28	11	726.84	279.26	<0.0001
A	642.01	1	642.01	246.66	<0.0001
B	1,233.39	1	1,233.39	473.87	<0.0001
C	5,978.74	2	2,989.37	1,148.53	<0.0001
AB	0.0208	1	0.0208	0.0080	0.9296
AC	42.19	2	21.10	8.11	0.0025
BC	60.86	2	30.43	11.69	0.0004
A^2	33.24	1	33.24	12.77	0.0018
B^2	13.35	1	13.35	5.13	0.0342
Residuals	54.66	21	2.60		
Lack of fit	48.13	15	1.09	2.95	0.0946
Pure error	6.53	6			
Cor Total	8,049.94	32			

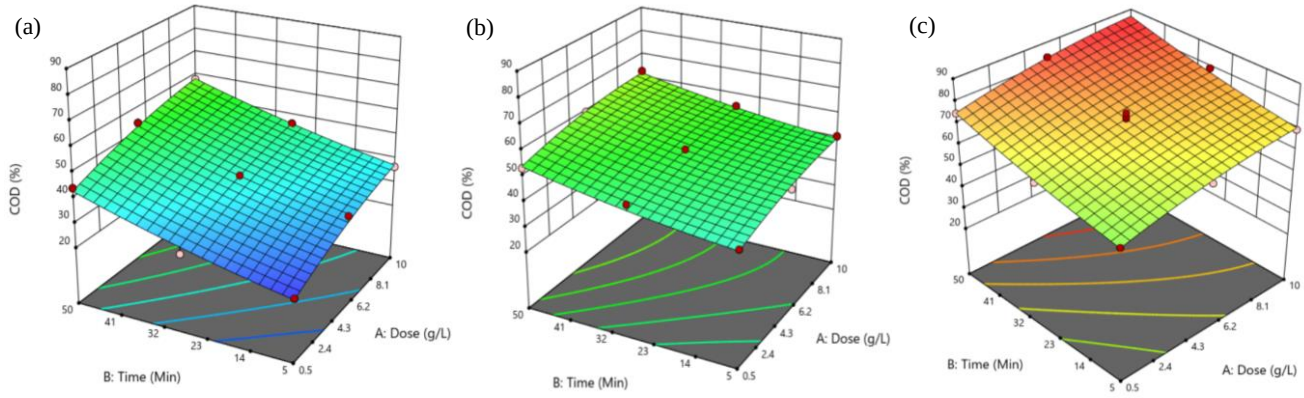

Figure 6. 3D Surface plot of PMCS biochar (a) 350, (b) 550 and (c) 800

3.6 Validation of the model results on real textile wastewater

To validate the CCD-RSM model, optimized conditions were applied to partially treated textile effluent (COD 200 mg/L and BOD 30 mg/L) from identified CETP of Ahmedabad. The optimized biochar (i.e., PCS800) was tested with 6.43 g/L of adsorbent dose and 33 min of mixing time at 150 rpm under batch adsorption and achieved 60% of COD reduction and >90% decolorization as shown in Figure 7.

Figure 7. Experimental photograph of treated real textile wastewater

The high efficiency for colour removal was due to chromophore part of dye adsorption, while COD reduction was achieved due to uptake of organic contaminants present in it. The treated effluent showed final COD<88 mg/L with complete colour removal. Unlike the synthetic wastewater, where the COD contributing components (EBT dye, starch and salts) are well defined, real textile wastewater contains unknown and variable dye mixtures, surfactants, sizing agents and auxiliary chemicals. Because different dyes exhibit different adsorption mechanisms and optimum pH ranges (Aritonang et al., 2025). The heterogeneity of the real effluent reduces the overall removal efficiency compared to the controlled synthetic matrix as reported in previous studies (Yaseen and Scholz, 2019; Castillo-Suárez et al., 2023). The COD removal performance of PMCS was compared with various biochar reported in literature Table 5.

Table 5. Recent studies on removal of chemical oxygen demand (COD) with biochar

Biochar	Feed stock modification	Wastewater type	% COD removal efficiency	References
Cotton Stalk	H_3PO_4-activated cotton stalk at 800°C	Textile wastewater	60	Present work
Walnut shell	Chemically activated with $FeCl_3$	Municipal wastewater	63.1	Rajabian et al. (2024)
Sugarcane baggase	Physical activation	Textile wastewater	55	da Costa et al. (2021)
Rice husk	$ZnCl_2$-activated rice husk	Wastewater	45.9	Mortada et al. (2023)
Corn stalk	$ZnCl_2$-activated corn stalk	Hospital wastewater	71.4	Walanda et al. (2022)
Lemon peels	$ZnCl_2$-activated at 800°C	Oil palm wastewater	82.72	Ahmad Ridzuan et al. (2025)
Tea waste	H_3PO_4 treated and H_2O_2 oxidized	Produced water	95.5	Khurshid et al. (2021a)

Previous studies show that COD removal using biochar varies widely, generally between 45-95%, depending on feedstock, activation method, and wastewater complexity. Activated sugarcane bagasse and rice-husk biochar achieved 55% and 45.9% COD removal in textile and industrial wastewater, respectively, while $FeCl_3$-activated walnut shell biochar reached 63.1% in municipal wastewater. Although highly modified systems such as tea waste biochar achieved 95.5% removal in produced water, these were tested on less complex matrices. In comparison, the 60% COD removal obtained with PMCS in real textile wastewater is competitive and aligns with the range reported for real, multi-component wastewaters, confirming the suitability of PMCS under practical treatment conditions. Hence, application of PMC treated effluent is safe for discharge and suitable for reuse when combined with advanced treatments like ultrafiltration (UF) or reverse osmosis (RO).

3.7 Isotherm results

The Langmuir and Freundlich adsorption isotherms of PCS350, PCS550, and PCS800 for % COD removal are shown in Figure 8(a-f). The corresponding isotherm constants are summarized in Table 6.

As shown in the Figure 8(a) for the PCS350, Langmuir fit was poor (R^2=0.7521, q_{max}=183.8 mg/g, K_L=0.0024 L/mg), indicating non-uniform adsorption, whereas Freundlich fit was stronger (R^2=0.9573, K_f=1.43 $mg^{-1}\frac{1}{n} \times L\frac{1}{n}.g^{-1}$ n=1.42) as shown in Figure 8(d), confirming favourable multilayer adsorption via electrostatic attraction, H-bonding and pore filling. For PCS550, Langmuir gave R^2=0.8864 with q_{max}=126.1 mg/g, K_L=0.0061 L/mg (Figure 8(b)), while Freundlich showed better correlation (R^2=0.8663, K_f=4.46 $mg^{-1}\frac{1}{n} \times L\frac{1}{n}.g^{-1}$, n=1.93) Figure 8(e), again suggesting heterogeneous adsorption, consistent with cotton stalk biochar reported by (Gao et al., 2021). In contrast, PCS800 fitted best to Langmuir (R^2=0.9994, q_{max}=90.2 mg/g, K_L=0.049 L/mg) as per Figure 8(c), while Freundlich (K_f=32.2 $mg^{-1}\frac{1}{n} \times L\frac{1}{n}.g^{-1}$, n=5.52, R^2=0.8715) also confirmed favourable adsorption as per Figure 8(f).

Table 6. Summary of isotherm constants

Biochar	Langmuir constants			Freundlich Constants		
	q_{max} (mg/L)	K_L (L/mg)	R^2	K_f ($mg^{-1} \cdot L \cdot g^{-1}$)	n	R^2
PCS350	183.8	0.0024	0.7521	1.43	1.42	0.9573
PCS550	126.1	0.0061	0.8864	4.46	1.93	0.8663
PCS800	90.2	0.0490	0.9994	32.2	5.52	0.8715

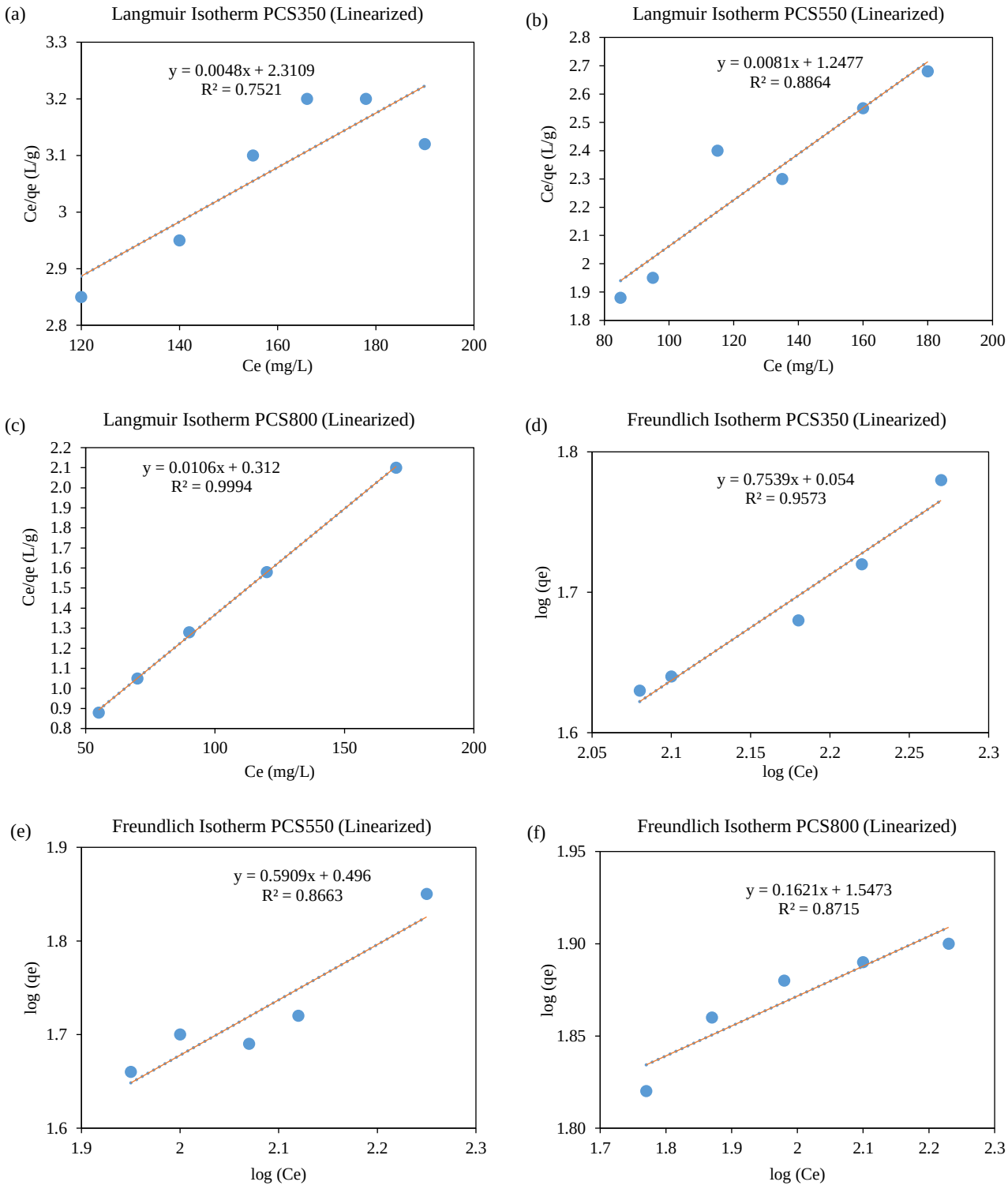

Figure 8. Adsorption isotherm at varied temperatures Langmuir at (a) 350°C, (b) 550°C, (c) 800°C; Freundlich at (d) 350°C, (e) 550°C, (f) 800°C

This transition can be attributed to the development of surface chemistry and porosity with pyrolysis temperature (Park et al., 2019). At 350°C, the biochar surface contains abundant oxygenated groups (-COOH, -OH) and a highly disordered carbon matrix, which produce heterogeneous surface energies capable of interacting with a wide spectrum of organic molecules. This explains the higher Langmuir q_{max} of PCS350, as these polar sites readily bind both EBT dye and larger macromolecular components i.e. starch through hydrogen bonding, electrostatic attraction and weak van der Waals forces. At 550°C, partial aromatization and moderate pore development create a balance of polar and aromatic domains, supporting mixed adsorption processes and resulting in intermediate q_{max} and model behaviour. In contrast, PCS800 exhibits highly aromatized carbon, greatly reduced surface polarity and well developed microporosity, favouring uniform monolayer adsorption through π-π interactions and hydrophobic effects. These interactions strongly promote the uptake of smaller aromatic dye molecules such as EBT, while the reduced number of polar sites and narrower pores restrict adsorption of bulky starch molecules, explaining the lower q_{max} but higher K_L observed for PCS800. This progressive shift in adsorption pathway from heterogeneous multilayer adsorption to uniform monolayer adsorption is fully consistent with the kinetic trend (PFO → PSO) and reflects increasing structural refinement and selectivity with pyrolysis temperature.

3.8 Kinetic results

The kinetic behaviour of COD adsorption onto PCS350, PCS550, and PCS800 was evaluated using the pseudo first order (PFO) and pseudo second order (PSO) models. These models help to determine whether the rate controlling step is primarily diffusion controlled or surface-interaction controlled. The Figure 9 showed the kinetic fit while Table 7 summarizes the fitted kinetic parameters.

Table 7. Summary of fitted kinetic parameters

Biochar	Pseudo first order (PFO) fitted parameters			Pseudo second order (PSO) fitted parameters		
	q_e (mg/g)	k_1 (min^{-1})	R^2	q_e (mg/g)	k_2 (g/mg·min)	R^2
PCS350	24	0.0582	0.988	24	2.54×10^{-3}	0.988
PCS550	29.6	0.0755	0.976	--	3.35×10^{-3}	0.995
PCS800	--	0.0814	0.976	30	3.41×10^{-3}	0.994

For PCS350, an initial rapid phase lasting 30-45 min was followed by equilibrium at around 60-90 min (q_e≈24 mg/g). PFO fit slightly better (R^2=0.988, k_1=0.0582 min^{-1}) than PSO (R^2=0.988, $k_2=2.54\times10^{-3}$ g/mg·min), indicating diffusion-controlled physisorption on a heterogeneous surface, consistent with earlier low-temperature biochar where external diffusion dominates.

The results of the PFO and PSO kinetic results for COD uptake onto PMCSB at varied temperature (Jegan et al., 2020; Li et al., 2023). Similarly, for PCS550, COD reduction reached equilibrium at ~90 min with PSO showing superior fit (R^2=0.995, q_e=29.6 mg/g, $k_2=3.35\times10^{-3}$ g/mg·min) compared to PFO (R^2=0.976, k_1=0.0755 min^{-1}). This indicates stronger surface interactions and site-specific adsorption, in agreement with previous COD adsorption studies on biochar (Dada et al., 2021; Khurshid et al., 2021b; Patel, 2024)

PCS800 exhibited the highest capacity (q_e=30 mg/g) and equilibrium at ~120 min. PSO fitted best (R^2=0.994, $k_2=3.41\times10^{-3}$ g/mg·min), while PFO fit was weaker (R^2=0.937). The dominance of PSO at higher temperature reflects increased aromaticity, pore development, and specific binding, as similarly reported for 800°C biochar from soybean straw and orange peel.

Overall, the adsorption behaviour across PCS350, PCS550, and PCS800 reflects the progressive structural evolution of biochar with increasing pyrolysis temperature. PCS350, rich in oxygenated functional groups and possessing limited porosity, exhibits diffusion-controlled physisorption and heterogeneous multilayer adsorption, consistent with its PFO and Freundlich fits. As temperature increases to 550°C, partial aromatization and moderate pore development introduce a balance of polar and aromatic sites, yielding mixed kinetic behaviour but a stronger PSO fit due to the emergence of more reactive adsorption sites. PCS800, characterized by extensive aromatization, reduced surface polarity and well-developed microporosity,

supports uniform, site-specific adsorption dominated by π-π and hydrophobic interactions, which aligns with its strong Langmuir and PSO fits. Thus, the transition from PFO to PSO and Freundlich to Langmuir is a direct consequence of increasing aromaticity, pore accessibility and the loss of surface oxygenated groups during pyrolysis (Elnour et al., 2019; Tomczyk et al., 2020). Similarly low cost biochar such as rice husk, tea waste and biogas residue derived biochar reported the same trend for COD removal by Langmuir behaviour and pseudo second order which can be explained by chemisorption rather than physical forces of adsorption (Khurshid et al., 2021a; Mortada et al., 2023; Wang et al., 2023).

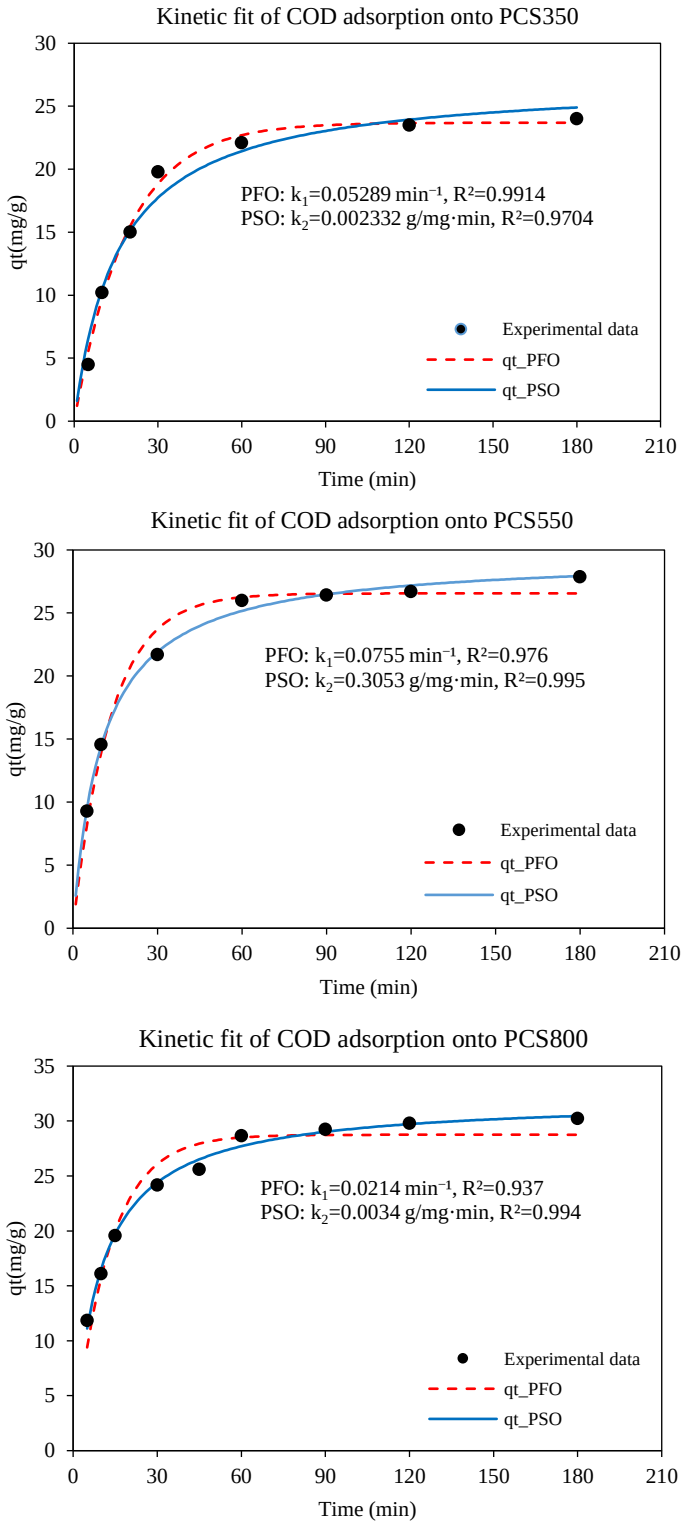

Figure 9. Kinetic fit graphs for PFO and PSO of (a) PCS350, (b) PCS550, (c) PCS80

3.9 Proposed adsorption mechanism in multi component synthetic wastewater

As the synthetic wastewater contains EBT dye, starch, and dissolved salts, the adsorption behaviour must be interpreted in a multi-component context. EBT, an anionic aromatic dye, binds preferentially to PCS550 and PCS800 through π-π stacking, hydrophobic interactions, and electrostatic attraction when pH < pHpzc, owing to their more developed aromatic domains. Similar interaction pathways have been reported for EBT adsorption onto carbonaceous materials, where monolayer adsorption on aromatic surfaces and strong dye carbon affinity were observed for activated carbon derived from rice hulls (de Luna et al., 2013). Likewise, tea-waste biochar has shown that π-π stacking, hydrophobic forces, van der Waals interactions, and pH-dependent electrostatic effects govern EBT uptake, with equilibrium behaviour following Langmuir and kinetics following pseudo-second-order models (Bansal et al., 2020). These literature results are consistent with the interaction mechanisms proposed for PMCS.

In contrast to EBT, starch being a large non-aromatic polysaccharide adsorbs mainly through hydrogen bonding and pore entrapment and therefore shows higher uptake on PCS350, which retains abundant oxygenated functional groups and larger accessible pores. The salts present (NaCl, Na_2CO_3, $NaHCO_3$) influence ionic strength and partially shield surface charges, reducing electrostatic interactions while enhancing hydrophobic pathways.

The pHpzc values of PCS350, PCS550, and PCS800 (5.8, 6.2, and 6.7) indicated in Figure 10, that at the operating pH 7 all surfaces are weakly negative. This behaviour aligns with (Ndoun et al., 2023), who reported that lignocellulosic biochar remain negatively charged over environmentally relevant pH ranges, with zeta potential becoming more negative as pH increases and typical pHpzc values below 4. Their findings support the interpretation that at neutral pH, electrostatic repulsion toward anionic dyes such as EBT is expected, making π-π and hydrophobic interactions the dominant pathways for adsorption.

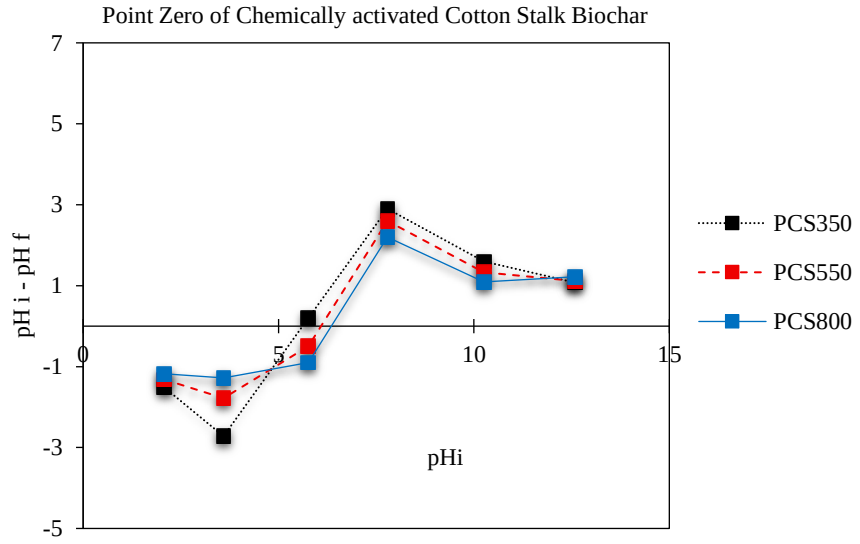

Figure 10. Point of zero charge graph of PCS350, PCS550, and PCS800

Hence, adsorption of EBT in this multi-component matrix is governed mainly by π-π stacking, hydrophobic attraction, and localized electrostatic interactions, whereas starch removal relies on polar functional groups. This selective and competitive site occupation explains why PCS800 shows higher affinity (high KL) despite lower q_{max}, while PCS350 exhibits higher theoretical capacity but weaker specific binding. These interaction pathways are summarised in Figure 11, which provides a graphical representation of the proposed adsorption mechanism. At higher temperature pore development and partial aromatization enhance pore filling and mixed interactions.

At 800°C, stabilized phosphate functionalities provide acidic sites, while graphitic domains favour π-π stacking and hydrophobic interactions, consistent with Langmuir monolayer adsorption and pseudo-second-order kinetics. Thus, synergistic effects of surface chemistry and pore structure govern COD reduction by PMCS.

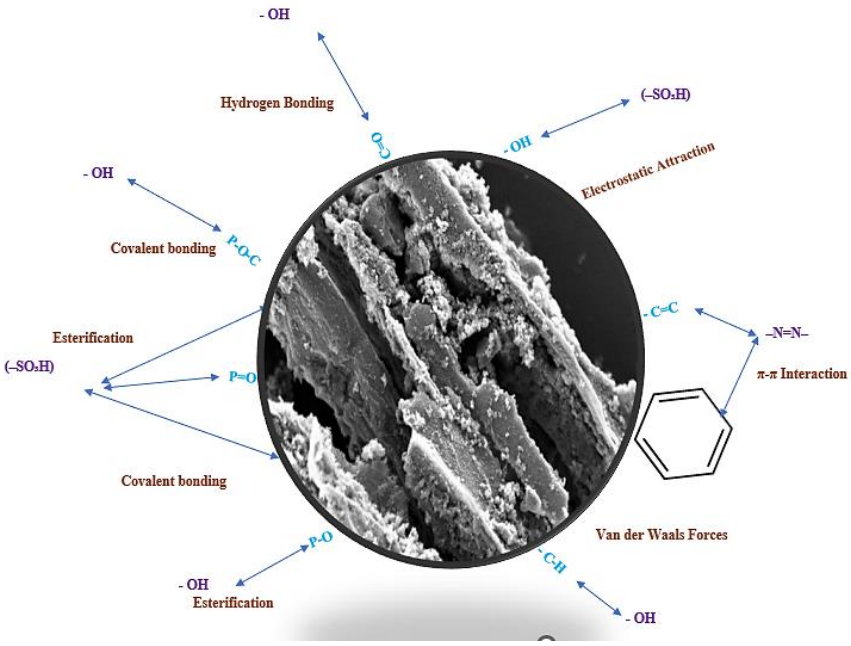

Figure 11. Possible mechanism of PCS800 in multi component synthetic wastewater

4. CONCLUSION

This study demonstrates a scalable circular economy pathway for converting cotton stalk into phosphate modified biochar (PMCS) and relates pyrolysis temperature to COD removal from textile wastewater. Using Central Composite Design, optimization revealed that adsorption shifted from heterogeneous multilayer behaviour at 350-550°C (best described by Freundlich, R^2=0.85-0.95) to uniform monolayer adsorption at 800°C (Langmuir, R^2=0.999). Kinetic analysis showed pseudo-first-order control at 350°C (k_1=0.0582 min^{-1}) and pseudo-second-order at 550-800°C (k_2=0.0033-0.0034 g/mg·min; R^2=0.994-0.995). Optimization achieved 76.7% COD reduction with PCS800 at pH 7, dose 6.43 g/L, and 33 min mixing, attributed to micropore driven uptake, while PCS550 offered the most balanced removal of small and large organics. The transition in behaviour reflects progressive aromatization, micropore development, and loss of labile oxygen groups with increasing temperature. Practically, PCS550 is recommended for treating complex effluents, whereas PCS800 is suited for polishing applications. Future work should extend this framework to column studies, regeneration, and techno-economic assessment to fully establish circular economy benefits. Overall, phosphate modification of cotton stalk biochar provides a technically rigorous and sustainable route for textile wastewater treatment, aligning waste valorization with environmental protection.

ACKNOWLEDGEMENTS

The authors sincerely acknowledge Central University, Gandhinagar for providing the laboratory facilities and support in conducting SEM and FTIR analyses, which were essential for this research work. The authors also thank the faculty members of the Department of Environmental Engineering, L.D. College of Engineering for their continuous encouragement, valuable suggestions, and support throughout the study.

AUTHOR CONTRIBUTIONS

Vishwa Vraj Shah, Ph.D. scholar, contributed to the conceptualization of the study, adoption of methodology, execution of research work, and preparation of the manuscript. Dr. Narendra Madhavlal Patel reviewed the manuscript and provided critical suggestions for its improvement.

DECLARATION OF CONFLICT OF INTEREST

The authors declare no conflict of interest.

REFERENCES

Agyemang E, Ofori-Dua K, Dwumah P, Forkuor JB. Towards responsible resource utilization: A review of sustainable vs. unsustainable reuse of wood waste. PLoS One 2024;19(12):e0312527.

Ahmad I, Farwa U, Khan ZUH, Imran M, Khalid MS, Zhu B, et al. Biosorption and health risk assessment of arsenic contaminated water through cotton stalk biochar. Surfaces and Interfaces 2022;29:Article No. 101806.

Ahmad Ridzuan NAN, Kasmuri N, Hamid KA, Nayono SE, Mojiri A, Selim H, et al. Remediation of palm oil mill effluent using citrus peel–based activated carbon. IOP Conference Series: Earth and Environmental Science 2025;1548:Article No. 1012030.

Ali J, Bakhsh EM, Hussain N, Bilal M, Akhtar K, Fagieh TM, et al. A new biosource for synthesis of activated carbon and its potential use for removal of methylene blue and eriochrome black T from aqueous solutions. Industrial Crops and Products 2022;179:Article No. 114676.

Arampatzidou AC, Voutsa D, Deliyanni EA, Matis KA. Adsorption of endocrine disruptor bisphenol A by carbonaceous materials: Influence of their porosity and specific surface area. Desalin Water Treat 2017;76:232-40.

Aritonang B, Ritonga AH, Harefa K, Herlina H. Reduction of BOD, COD, and TSS in textile wastewater using bentonite activated charcoal adsorbent. Jurnal Farmsimed 2025;7:381-9.

Arous F, Pinelli D, Bessadok S, Boudagga S, Hamdi C, Li W, et al. Performance and cost-benefit analyses of an integrated process for advanced treatment of highly saline textile wastewater at a semi-industrial scale. Euro-Mediterranean Journal for Environmental Integration 2024;9:605-20.

Bansal M, Patnala PK, Dugmore T. Adsorption of eriochrome Black-T(EBT) using tea waste as a low cost adsorbent by batch studies: A green approach for dye effluent treatments. Current Research in Green and Sustainable Chemistry 2020;3:Article No. 100036.

Beyan SM, Prabhu SV, Sissay TT, Getahun AA. Sugarcane bagasse based activated carbon preparation and its adsorption efficacy on removal of BOD and COD from textile effluents: RSM based modeling, optimization and kinetic aspects. Bioresource Technology Reports 2021;14:Article No. 100664.

Bhuvaneshwari S, Hettiarachchi H, Meegoda JN. Crop residue burning in India: Policy challenges and potential solutions. International Journal of Environmental Research and Public Health 2019;16(5):Article No. 832.

Castillo-Suárez LA, Sierra-Sánchez AG, Linares-Hernández I, Martínez-Miranda V, Teutli-Sequeira EA. A critical review of textile industry wastewater: Green technologies for the removal of indigo dyes. International Journal of Environmental Science and Technology 2023;20:10553-90.

Colmenares JC, Varma RS, Lisowski P. Sustainable hybrid photocatalysts: Titania immobilized on carbon materials derived from renewable and biodegradable resources. Green Chemistry 2016(21);18:5736-50.

da Costa WKOC, Gavazza S, Duarte MMMB, Freitas SKB, de Paula NTG, Paim APS. Preparation of activated carbon from sugarcane bagasse and removal of color and organic matter from Real Textile Wastewater. Water, Air, and Soil Pollution 2021;232:Article No. 358.

Cui Q, Huang Y, Ma X, Li S, Bai R, Li H, et al. Research on the adsorption mechanism and performance of cotton stalk-based biochar. Molecules 2024;29(24):Article No. 5841.

Dada AO, Adekola FA, Odebunmi EO, Ogunlaja AS, Bello OS. Two-three parameters isotherm modeling, kinetics with statistical validity, desorption and thermodynamic studies of adsorption of Cu(II) ions onto zerovalent iron nanoparticles. Scientific Reports 2021;11:Article No. 16454.

Deshpande MV, Kumar N, Pillai D, Krishna VV, Jain M. Greenhouse gas emissions from agricultural residue burning have increased by 75% since 2011 across India. Science of the Total Environment 2023;904:Article No. 166944.

Dhanya MS. Perspectives of agro-waste biorefineries for sustainable biofuels. In: Nandabalan YK, Garg VK, Labhsetwar NK, Singh A, editors. Zero Waste Biorefinery. Energy, Environment, and Sustainability. Singapore: Springer; 2022. p. 207-32.

Díaz B, Sommer-Márquez A, Ordoñez PE, Bastardo-González E, Ricaurte M, Navas-Cárdenas C. Synthesis methods, properties, and modifications of biochar-Based materials for wastewater treatment: A review. Resources 2024;13:Article No. 8.

Dowlatshah S, Hay AO, Noreng L, Hansen FA. A practical tutorial for optimizing electromembrane extraction methods by response surface methodology. Advances in Sample Preparation 2025;14:Article No. 100170.

Du K-Q, Li J-F, Farid MA, Wang W-H, Yang G. Preparation of high-efficient phosphoric acid modified biochar toward ciprofloxacin removal from wastewater. Industrial Crops and Products 2025;226:Article No. 120649.

Elnour AY, Alghyamah AA, Shaikh HM, Poulose AM, Al-Zahrani SM, Anis A, et al. Effect of pyrolysis temperature on biochar microstructural evolution, physicochemical characteristics, and its influence on biochar/polypropylene composites. Applied Sciences 2019;9:Article No. 1149.

Gao L, Li Z, Yi W, Li Y, Zhang P, Zhang A, et al. Impacts of pyrolysis temperature on lead adsorption by cotton stalk-derived biochar and related mechanisms. Journal of Environmental Chemical Engineering 2021;9(4):Article No. 105602.

Grover D, Chaudhry S. Ambient air quality changes after stubble burning in rice-wheat system in an agricultural state of India. Environmental Science and Pollution Research 2019;26:20550-9.

He M, Xu Z, Hou D, Gao B, Cao X, Ok YS, et al. Waste-derived biochar for water pollution control and sustainable development. Nature Reviews Earth and Environment 2022;3:444-60.

Heidarinejad Z, Dehghani MH, Heidari M, Javedan G, Ali I, Sillanpää M. Methods for preparation and activation of activated carbon: A review. Environmental Chemistry Letters 2020;18:393-415.

Hussain M, Imran M, Abbas G, Shahid M, Iqbal M, Naeem MA, et al. A new biochar from cotton stalks for As (V) removal from aqueous solutions: its improvement with H_3PO_4 and KOH. Environmental Geochemistry and Health 2020;42:2519-34.

Jegan J, Praveen S, Bhagavathi Pushpa T, Gokulan R. Sorption kinetics and isotherm studies of cationic dyes using groundnut (*Arachis hypogaea*) shell derived biochar a low-cost adsorbent. Applied Ecology and Environmental Research 2020;18(1):1925-39.

Kamran U, Bhatti HN, Noreen S, Tahir MA, Park S-J. Chemically modified sugarcane bagasse-based biocomposites for efficient removal of acid red 1 dye: Kinetics, isotherms, thermodynamics, and desorption studies. Chemosphere 2022;291:Article No. 132796.

Khalid U, Inam MA. The influence of pyrolysis temperature on the performance of cotton stalk biochar for hexavalent chromium removal from wastewater. Water, Air, and Soil Pollution 2024;235:Article No. 114.

Khan H, Hussain S, Hussain SF, Gul S, Ahmad A, Ullah S. Multivariate modeling and optimization of Cr(VI) adsorption onto carbonaceous material via response surface models

assisted with multiple regression analysis and particle swarm embedded neural network. Environmental Technology and Innovation 2021;24:Article No. 101952.

Khurshid H, Mustafa MRU, Rashid U, Isa MH, Ho YC, Shah MM. Adsorptive removal of COD from produced water using tea waste biochar. Environmental Technology and Innovation 2021a;23:Artilce No. 101563.

Khurshid H, Mustafa MRU, Rashid U, Isa MH, Ho YC, Shah MM. Adsorptive removal of COD from produced water using tea waste biochar. Environmental Technology and Innovation 2021b;23:Article No. 101563.

Kwarciak-Kozłowska A, Fijałkowski KL. Efficiency assessment of municipal landfill leachate treatment during advanced oxidation process (AOP) with biochar adsorption (BC). Journal of Environmental Management 2021;287:Article No. 112309.

Li L, Zhang H, Liu Z, Su Y, Du C. Adsorbent biochar derived from corn stalk core for highly efficient removal of bisphenol A. Environmental Science and Pollution Research 2023;30(30):74916-27.

Li T, Li J-P, Li Z-P, Cheng X-W. Eco-friendly modified biochar for phosphate removal: Adsorption mechanism and application in pressed vegetable wastewater treatment. Environmental Engineering Science 2024a;41:401-12.

Li R, Zhang C, Hui J, Shen T, Zhang Y. The application of P-modified biochar in wastewater remediation: A state-of-the-art review. Science of the Total Environment 2024b;917:Article No. 170198.

Liu Q, Li D, Cheng H, Cheng J, Du K, Hu Y, et al. High mesoporosity phosphorus-containing biochar fabricated from Camellia oleifera shells: Impressive tetracycline adsorption performance and promotion of pyrophosphate-like surface functional groups (C-O-P bond). Bioresource Technology 2021;329:Article No. 124922.

Liu T, Fan X, Wu K, Tao C, Bai X, Sun X. Structural characteristics of biochars made from different parts of corn straw and their adsorption performances for methylene blue. Journal of Water Process Engineering 2024;68:Article No. 106562.

de Luna MDG, Flores ED, Genuino DAD, Futalan CM, Wan M-W. Adsorption of Eriochrome Black T (EBT) dye using activated carbon prepared from waste rice hulls—Optimization, isotherm and kinetic studies. Journal of the Taiwan Institute of Chemical Engineers 2013;44:646-53.

Manzar MS, Khan G, dos Santos Lins PV, Zubair M, Khan SU, Selvasembian R, et al. RSM-CCD optimization approach for the adsorptive removal of Eriochrome Black T from aqueous system using steel slag-based adsorbent: Characterization, Isotherm, Kinetic modeling and thermodynamic analysis. Journal of Molecular Liquids 2021;339:Article No. 116714.

Mortada W, Mohamed R, Monem A, Awad M, Hassan A. Effective and low-cost adsorption procedure for removing chemical oxygen demand from wastewater using chemically activated carbon derived from rice husk. Separations 2023;10:Article No. 43.

Muhammad A, Shafeeq A, Butt MA, Rizvi ZH, Chughtai MA, Rehman S. Decolorization and removal of cod and bodfrom raw and biotreated textile dye bath effluent through advanced oxidation processes (AOPS). Brazilian Journal of Chemical Engineering 2008;25:453-9.

Muzyka R, Misztal E, Hrabak J, Banks SW, Sajdak M. Various biomass pyrolysis conditions influence the porosity and pore size distribution of biochar. Energy 2023;263:Article No. 126128.

Ndoun MC, Knopf A, Preisendanz HE, Vozenilek N, Elliott HA, Veith TL, et al. Physicochemical characterization of biochar derived from the pyrolysis of cotton gin waste and walnut shells. Journal of the American Society of Agricultural and Biological Engineers 2023;66:1163-74.

Okafor CC, Madu CN, Ajaero CC, Ibekwe JC, Nzekwe CA. Sustainable management of textile and clothing. Clean Technologies and Recycling 2021;1(1):70-87.

Ou W, Lan X, Guo J, Cai A, Liu P, Liu N, et al. Preparation of iron/calcium-modified biochar for phosphate removal from industrial wastewater. Journal of Cleaner Production 2023;383:Article No. 135468.

Oyekanmi AA, Ahmad A, Hossain K, Rafatullah M. Adsorption of Rhodamine B dye from aqueous solution onto acid treated banana peel: Response surface methodology, kinetics and isotherm studies. PLoS One 2019;14:e0216878.

Park J-H, Wang JJ, Meng Y, Wei Z, DeLaune RD, Seo D-C. Adsorption/desorption behavior of cationic and anionic dyes by biochars prepared at normal and high pyrolysis temperatures. Colloids and Surfaces A: Physicochemical and Engineering 2019;572:274-82.

Patel H. Removal of COD, BOD and color of different industrial effluents using activated neem char. Environmental Advances 2024;16:Article No. 100553.

Rajabian E, Sharififard H, Bonyadi M, Boostani F, Moradialvand M. COD reduction of municipal wastewater using mesoporous walnut shell-activated carbon: One step synthesis-modification via chemical activation with $FeCl_3$. Biomass Conversion and Biorefinery 2024;14:30627-40.

Roy H, Prantika TR, Riyad M, Paul S, Islam MS. Synthesis, characterizations, and RSM analysis of Citrus macroptera peel derived biochar for textile dye treatment. South African Journal of Chemical Engineering 2022;41:129-39.

Sadeghi S, Zakeri HR, Saghi MH, Ghadiri SK, Talebi SS, Shams M, et al. Modified wheat straw-derived graphene for the removal of Eriochrome Black T: Characterization, isotherm, and kinetic studies. Environmental Science and Pollution Research 2021;28:3556-65.

Sathya K, Nagarajan K, Carlin Geor Malar G, Rajalakshmi S, Raja Lakshmi P. A comprehensive review on comparison among effluent treatment methods and modern methods of treatment of industrial wastewater effluent from different sources. Applied Water Science 2022;12:Article No. 70.

Shah AJ, Soni B, Karmee SK. Application of cotton stalk biochar as a biosorbent for the removal of malachite green and its microwave-assisted regeneration. Energy, Ecology and Environment 2022;7:88-96.

Shao M, Ding ZC, Yang YZ, Zhang ZP, Wan YS. Phosphoric acid-modified biochar enhances electrokinetic in situ leaching technology to remediate Pb^{2+} contaminated soil. International Journal of Environmental Science and Technology 2024;21:8507-18.

Soleimani H, Sharafi K, Amiri Parian J, Jaafari J, Ebrahimzadeh G. Acidic modification of natural stone for Remazol Black B dye adsorption from aqueous solution- central composite design (CCD) and response surface methodology (RSM). Heliyon 2023;9(4):e14743.

Srivastav AL, Rani L, Sharda P, Patel A, Patel N, Chaudhary VK. Sustainable biochar adsorbents for dye removal from water:

present state of art and future directions. Adsorption 2024;30:1791-804.

Susaimanickam A, Manickam P, Joseph AA. A Comprehensive review on RSM-Coupled optimization techniques and its applications. Archives of Computational Methods in Engineering 2023;30:4831-53.

Tan W-T, Zhou H, Tang S-F, Zeng P, Gu J-F, Liao B-H. Enhancing Cd(II) adsorption on rice straw biochar by modification of iron and manganese oxides. Environmental Pollution 2022;300:Article No. 118899.

Tomczyk A, Sokołowska Z, Boguta P. Biochar physicochemical properties: Pyrolysis temperature and feedstock kind effects. Reviews in Environmental Science and Bio/Technology 2020;19:191-215.

Tzanakakis VA, Capodaglio AG, Angelakis AN. Insights into global water reuse opportunities. Sustainability 2023;15(17):Article No. 13007.

Vakili A, Zinatizadeh AA, Rahimi Z, Zinadini S, Mohammadi P, Azizi S, et al. The impact of activation temperature and time on the characteristics and performance of agricultural waste-based activated carbons for removing dye and residual COD from wastewater. Journal of Cleaner Production 2023;382:Article No. 134899.

Venkatesan A, Srividhya B, Alajmi A, Sadeq AM, Chava RK, Habila MA, et al. High adsorption capacities of rhodamine B dye by activated carbon synthesized from cotton stalks agricultural waste by chemical activation. Ceramics International 2025;51(10):13345-54.

Walanda DK, Anshary A, Napitupulu M, Walanda RM. The utilization of corn stalks as biochar to adsorb BOD and COD in hospital wastewater. International Journal of Design and Nature and Ecodynamics 2022;17:113-8.

Wang M, Wang G, Qian L, Yong X, Wang Y, An W, et al. Biochar production using biogas residue and their adsorption of ammonium nitrogen and chemical oxygen demand in wastewater. Biomass Convers Biorefinery 2023;13:3881-92.

Wu S, Wu H. Incorporating biochar into wastewater eco-treatment systems: Popularity, reality, and complexity. Environmental Science and Technology 2019;53:3345-6.

Xiang W, Zhang X, Cao C, Quan G, Wang M, Zimmerman AR, et al. Microwave-assisted pyrolysis derived biochar for volatile organic compounds treatment: Characteristics and adsorption performance. Bioresource Technology 2022;355:Article No. 127274.

Xu J, Fu M, Ma Q, Zhang X, You C, Shi Z, et al. Modification of biochar by phosphoric acid via wet pyrolysis and using it for adsorption of methylene blue. RSC Advances 2023;13(22): 15327-33.

Xu Q, Li C, Sumita, Pang W. Study on the removal efficacy and mechanism of phosphorus from wastewater by eggshell-modified biochar. Water Environment Research 2024;96(3): e10998.

Yaseen DA, Scholz M. Textile dye wastewater characteristics and constituents of synthetic effluents: a critical review. International Journal of Environmental Science and Technology 2019;16:1193-226.

Yusuff AS, Ishola NB, Gbadamosi AO, Epelle EI. Modeling and optimization of hexavalent chromium adsorption by activated eucalyptus biochar using response surface methodology and adaptive neuro-fuzzy inference system. Environments 2023;10(3):Article No. 55.

Zafar S, Razzaq A, Khalid S, Tariq TZ, Fatima R, Rabbani F, et al. Recent Advances in Applications of Engineered Biochar for Wastewater Treatment. In: Catalytic Applications of Biochar for Environmental Remediation: A Green Approach Towards Environment Restoration (Vol. 1). American Chemical Society Pubilcations; 2024. p. 109-30.

Zeng X-Y, Wang Y, Li R-X, Cao H-L, Li Y-F, Lü J. Impacts of temperatures and phosphoric-acid modification to the physicochemical properties of biochar for excellent sulfadiazine adsorption. Biochar 2022;4:Article No. 14.

Zeng Y, Lin Y, Ma M, Chen H. A review on the removal of heavy metals from water by phosphorus-enriched biochar. Minerals 2024;14(1):Article No. 61.

Zhao A, Liu S, Yao J, Huang F, He Z, Liu J. Characteristics of bio-oil and biochar from cotton stalk pyrolysis: Effects of torrefaction temperature and duration in an ammonia environment. Bioresource Technology 2022;343:Article No. 126145.

Zhao L, Zheng W, Mašek O, Chen X, Gu B, Sharma BK, et al. Roles of phosphoric acid in biochar formation: Synchronously improving carbon retention and sorption capacity. Journal of Environmental Quality 2017;46 (2):393-401.

Zhou F, Li K, Hang F, Zhang Z, Chen P, Wei L, et al. Efficient removal of methylene blue by activated hydrochar prepared by hydrothermal carbonization and NaOH activation of sugarcane bagasse and phosphoric acid. RSC Advances 2022;12(3): 1885-96.

Zhu X, Labianca C, He M, Luo Z, Wu C, You S, et al. Life-cycle assessment of pyrolysis processes for sustainable production of biochar from agro-residues. Bioresource Technology 2022;360:Article No. 127601.